18th International Conference on Information Fusion
Washington, DC - July 6-9, 2015

Fault detection and exclusion of cycle slips for carrier-phase in GNSS positionning

M. Kaddour[1,2], N. Aït Tmazirte[1] and M. E. El Najjar[1]

[1]CRIStAL UMR 9189 CNRS/Université-Lille1/Ecole Centrale de Lille Villeneuve d'Ascq, France
mahmoud.kaddour@ed.univ-lille1.fr

Z.Naja[2,3] and N. Moubayed[2,3]

[2]Lebanese University, EDST, AZM platform for research in biotechnology, Tripoli, Lebanon

[3] Lebanese University, Faculty of Engineering 1, Tripoli, Lebanon

Abstract*— This paper presents an algorithm of a standalone GPS positioning system that uses both the C/A code and L1 carrier-phase measurements. The algorithm is based on a dynamic state vector estimation using Information Filter (IF) and information theory metrics. The GPS carrier-phase measurements suffer from a common error source which is the cycle slips (CS). To solve such a problem, i.e. the detection and exclusion of CS from the positioning algorithm, in this work, we propose to integrate a Fault Detection and Exclusion (FDE) level into the data fusion procedure. The proposed methodology consists of four stages. The first one is the marginalization step that is suitable to add or eliminate an element of state vector. The second stage is the prediction step of the IF. The third stage uses the proposed FDE method to detect and exclude the CS and other errors. At the end comes the update stage (correction stage). Finally, the algorithm is tested using real data acquired with an experimental vehicle using low cost GNSS receivers in order to demonstrate the efficiency and validity of the proposed method.

Keywords: GNSS, Marginalization, Information Filter, Information theory.

1 Introduction

Usually the carrier phase processing is used within the context of differential positioning with integer or float ambiguities [1]. In recent years, standalone GPS positioning algorithms using carrier phase processing with floating ambiguities has aroused attention for a several reasons: for example, it doesn't require base stations and it uses simplified operations with low costs [2]. The basic problem of the carrier phase is the CS. In literature, there are many shortages to solve such problem. For instance, the wavelet analysis can be used to test the availability of cycle slips [3][4]. Also, the Kalman filter [6] and the least squares [7] can be used to monitor the integrity of carrier phase that carry out the CS. Another method uses two steps, one to exclude large cycle slips and another for small cycle slips [5]. In this paper, the proposed method is based on information filter and information theory for data fusion and for the detection and exclusion of CS and faulty measurements.

The CS are discontinuities of an integer number of cycles in the measured carrier-phase resulting from a temporary loss-of-lock in the carrier tracking loop of a GPS receiver [4]. There are three sources of cycle slips. First of all, the CS are caused by obstructions of the satellite signal due to building, trees....The second cause is related to internal receiver tracking problems, reflected in a false signal processing. The third cause is a low Signal to Noise Ratio (SNR) due to extreme low satellite elevation.

The IF is the information form of the Kalman filter (KF), it uses an information vector and an information matrix (fisher matrix) to represent the state vector and the covariance matrix of KF. It is characterized, in term of computational costs, by a complex prediction step and a simple correction step. This helps to simplify the cycle slip and other fault measurements detection and to reduce the computational time [8][9][10]. In the proposed work, a marginalization stage is used to add or/and eliminate elements from the information vector and the information matrix. This stage ensures to conserve convergence of the system [11][12].

A new hierarchical architecture based on filters synthesis policy for Fault Detection and Exclusion (FDE) method is presented by using the IF and information theory metrics. In order to detect and to exclude faults measurement, a Log Likelihood Ratio (LLR) test based on Mutual Information (MI) is elaborated [12]. This LLR test is used to quantify the difference in term of certainty between a main IF filter and a set of sub-filters.

This paper is organized as follows. Section 2 develops and describes the measurement model, the observation model, marginalization, the information filter and the information quantification. Section 3 describes our work and the proposed algorithm (FDE method) and methodology. Section 4 presents tests and validations using real GPS measurement data in addition to the results and discussions. Finally, Section 5 provides conclusion and perspectives.

2 Information Filtering and Information Quantification

2.1 Measurement Model

The measurements used by the information filter are categorized as standalone receiver types. These include C/A code and L1 carrier-phase observations. Such measurement model is given by:

$$z = \begin{bmatrix} \rho \\ (\varphi + N)\lambda \\ \rho - \varphi\lambda \end{bmatrix} \quad (1)$$

Here N is the phase ambiguities , ρ and φ denote the set of pseudo range and carrier-phase for all observed satellites, ρ and $(\varphi + N)\lambda$ are the distance between the receiver sensor and the observation satellites plus clock range, and other errors types, $\rho - \varphi\lambda$ is the combination between the carrier-phase and the C/A code measurements used to compute ambiguities.

And the pseudo-range can be modeled as follow:

$$\begin{aligned} &\rho^{s_i} \\ &= \sqrt{\left(x_i^s - x_{pr}\right)^2 + \left(y_i^s - y_{pr}\right)^2 + \left(z_i^s - z_{pr}\right)^2} + \\ &\quad \delta\rho_{iono}^{s_i} - \delta\rho_{tropo}^{s_i} + c\left(\partial(k) - \partial^{si}(k)\right) \\ &= R_{pr}^{s_i} + \delta\rho_{iono}^{s_i} - \delta\rho_{tropo}^{s_i} + c\left(\partial(k) - \partial^{si}(k)\right) \end{aligned} \quad (2)$$

$\delta\rho_{iono}^{s_i}$ and $\delta\rho_{tropo}^{s_i}$ are also the models of the atmospheric errors, $\partial^{si}(k)$ is the satellite clock error.

$\delta\rho_{tropo}^{s_i}$ is estimated by the Saastamoinen algorithm [15], and $\delta\rho_{iono}^{s_i}$is calculated by equation (3). Indeed, it is admitted that the ionosphere delays for φ and ρ measurements have the same values but an opposite sign [1].

$$\delta\rho_{iono}^{s_i} = abs((\varphi + N)\lambda - \rho)/2 \quad (3)$$

2.2 Dynamic Model

Consider a system evolving under the hypotheses that the velocity between two periods is constant and the system has a linear form. The prediction of the state vector $X(k)$ is given by:

$$X(k) = F.X(k-1) \quad (4)$$

The state variables for standalone observation are the position, the clock range, the velocity, and the phase ambiguities.

$$X(k) = \begin{bmatrix} x(k), \dot{x}(k), y(k), \dot{y}(k), z(k), \dot{z}(k), \\ c\,\partial(k), c\,\dot{\partial}(k), N_1, \dots, N_n \end{bmatrix} \quad (5)$$

Where $[x(k), y(k), z(k)]$ are the sensor receiver Cartesian coordinate, $[\dot{x}(k), \dot{y}(k), \dot{z}(k)]$ receiver velocity components and $\left[c\,\partial(k), c\,\dot{\partial}(k)\right]$ the clock range and the clock drift, and $[N_1, \dots, N_n]$ the ambiguities.

The state transition matrix F is given by:

$$F = \begin{bmatrix} 1 & T & 0 & 0 & 0 & 0 & 0 & 0 & 0 \\ 0 & 1 & 0 & 0 & 0 & 0 & 0 & 0 & 0 \\ 0 & 0 & 1 & T & 0 & 0 & 0 & 0 & 0 \\ 0 & 0 & 0 & 1 & 0 & 0 & 0 & 0 & 0 \\ 0 & 0 & 0 & 0 & 1 & T & 0 & 0 & 0 \\ 0 & 0 & 0 & 0 & 0 & 1 & 0 & 0 & 0 \\ 0 & 0 & 0 & 0 & 0 & 0 & 1 & T & 0 \\ 0 & 0 & 0 & 0 & 0 & 0 & 0 & 1 & 0 \\ 0 & 0 & 0 & 0 & 0 & 0 & 0 & 0 & J_n \end{bmatrix} \quad (6)$$

Where T is the sample period (in our case 1 second), J_n is the $n \times n$ identity matrix and n is the number of observations.

2.3 Observation model

The observation model is nonlinear, it can be written as:

$$Z(k) = h\big(X(k), v(k)\big) \quad (7)$$

Such model should be linearized around the predicted state to obtain an observation matrix. The linearization facilitates significantly the correct calculation of satellite positioning:

$$H = [H_x \quad H_N] \quad (8)$$

$$H_N = -\lambda * J_n \quad (9)$$

$$H_x = \begin{bmatrix} \nabla H_{x_{pr}}^{x_1^s} & 0 & \nabla H_{y_{pr}}^{y_1^s} & 0 & \nabla H_{z_{pr}}^{z_1^s} & 0 & 1 & 0 \\ \vdots & \vdots & \vdots & \vdots & \vdots & \vdots & \vdots & \vdots \\ \nabla H_{x_{pr}}^{x_i^s} & 0 & \nabla H_{y_{pr}}^{y_i^s} & 0 & \nabla H_{z_{pr}}^{z_i^s} & 0 & 1 & 0 \\ \vdots & \vdots & \vdots & \vdots & \vdots & \vdots & \vdots & \vdots \\ \nabla H_{x_{pr}}^{x_n^s} & 0 & \nabla H_{y_{pr}}^{y_n^s} & 0 & \nabla H_{z_{pr}}^{z_n^s} & 0 & 1 & 0 \end{bmatrix} \quad (10)$$

With

$$\nabla H_{x_{pr}}^{x_i^s} = \frac{\partial R_{x_{pr}}^{x_i^s}}{\partial x} = -\frac{x_i^s - x_{pr}}{R_{pr}^{s_i}} \quad (1)$$

$$\nabla H_{y_{pr}}^{y_i^s} = \frac{\partial R_{y_{pr}}^{y_i^s}}{\partial y} = -\frac{y_i^s - y_{pr}}{R_{pr}^{s_i}} \quad (2)$$

$$\nabla H_{z_{pr}}^{z_i^s} = \frac{\partial R_{z_{pr}}^{z_i^s}}{\partial z} = -\frac{z_i^s - z_{pr}}{R_{pr}^{s_i}} \quad (3)$$

The coordinates $[x_i^s, y_i^s, z_i^s]$ of each observation satellite, are calculated by broadcasted ephemeris.

2.4 Marginalisation step

The Information vector y has dimensions that vary according to the number of observed satellites. Therefore, we need to apply a marginalization stage. This stage is the

operation of extraction and addition of variables from the information vector y. The IF is optimal in the case of a Gaussian distribution. In order to conserve this distribution on y we apply a marginalization step. Indeed, the sub-vectors of a Gaussian vector stay Gaussian [9] [13][14].

2.5 Information Filtering

An IF is adopted in this paper for positioning and computing phase ambiguities because of its efficiency, especially for applications with large number of states and observations. The IF is divided into two steps. In the first step, the filter computes a prediction value of the Information vector $\dot{y}(k)$ and the Information matrix $\dot{Y}(k)$. The following prediction equations are used:

$$M_k = [F^{-1}]^T Y(k-1) F^{-1} \tag{4}$$

$$C_k = M_k[M_k + Q_k^{-1}]^{-1}(11) \tag{5}$$

$$L_K = J_{n+8} - C_K \tag{6}$$

$$\dot{Y}(k) = L_K M_k L_k^T + C_k Q_k^{-1} C_k^T \tag{7}$$

$$\dot{y}(k) = L_K [F^T]^T \bar{y}(k-1) \tag{8}$$

Where Q is system noise [1].

In the second step (the updating step), the current observations are used to correct the predicted step in order to obtain a more accurate estimation.

The updated Information vector and the updated corresponding information matrix are now given by the following equations:

$$Y(k) = \dot{Y}(k) + H_k^T(i,:) R_k^{-1}(i,i) H_k(i,:) \tag{9}$$

$$y(k) = \dot{y}(k) + H_k^T(i,:) R_k^{-1}(i,i) z_k(i) \tag{10}$$

Where $Y(k)$ is the updated information matrix, $y(k)$ is the updated information vector and R the covariance of the observation noise [1].

2.6 Information Quantification

The elaborated LLR based on MI aims to quantify the certainty of the estimation provided by a main filter using the N available observations compared to certainty of estimation of each sub filter. Each sub-filter from the set of sub-filters uses a unique combination of N-1 observations.

In the Information theory, the MI metric can be adapted to measure this kind of quantity. The MI of two random variables is the measure of their mutual dependence. The MI $I(x,z)$ can be used to evaluate the impact of each measurement on the certainty of the IF.

$I(x,z)$ is defined in [10] as:

$$I(x,y) = E\left(ln\frac{p(x|z)}{p(x)}\right) \tag{11}$$

In [10] also, the MI for a multivariate Gaussian distribution is represented as half the log-determinant of the covariance.

$$I(x,z) = \frac{1}{2} ln \frac{|p(X)|}{|p(X|z)|} \tag{12}$$

The following equation (22) shows the direct relation between an estimation error and a determinant covariance matrix. Where (x,y) are the estimated positions and $(\hat{x},\hat{y})$ are the real positions. Note that we use only $cov(x,y)$ (without z and ambiguities components) to simplify the calculation.

$$det\big(cov(x,y)\big) = E(x-\hat{x})^2 * E(y-\hat{y})^2 - [E(y-\hat{y})(x-\hat{x})]^2 \tag{13}$$

Knowing that the information matrix is the inverse of the covariance matrix; therefore there exist a relation between the positioning error and the determinant of the information matrix. Referring to that relation and the likelihood test, we can elaborate the following residual equation based on the log likelihood ratio.

$$LLT_i^{\rho} = \frac{1}{2} ln \frac{\left|\dot{Y}(k) + \left[\sum_{\substack{j=1 \\ i\neq j}}^{N} I_j^{\rho}\right]\right|}{\left|\dot{Y}(k) + \sum_{j=1}^{N} I'_j\right|} \tag{14}$$

$$LLT_i^{\varphi} = \frac{1}{2} ln \frac{\left|\dot{Y}(k) + \left[\sum_{\substack{j=1 \\ i\neq j}}^{N} I_j^{\varphi}\right]\right|}{\left|\dot{Y}(k) + \sum_{j=1}^{N} I'_j\right|} \tag{15}$$

Where:

$$I_i^{\rho} = H_k^T(i,:) * \theta_i{}^{\rho} * H_k(i,:) \tag{16}$$

$$I_i^{\varphi} = H_k^T(i,:) * \theta_i{}^{\varphi} * H_k(i,:) \tag{17}$$

$$\theta_i^{\rho} = \left|\tilde{\rho}_r^{si} - \rho_r^{si}\right|^{-1} \tag{18}$$

$$\theta_i^{\varphi} = \left|\tilde{\rho}_r^{si} - \lambda(\varphi_r^{si} + N_r^{si})\right|^{-1} \tag{19}$$

θ_i^{ρ} is the estimation of the C/A code observation error, θ_i^{φ} is the estimation of the L1 phase observation error.

In conclusion, the likelihood ratio Test (LLT) computes the certainty of the potential corrected position estimation using the i_{th} set of observations.

3 Proposed Methodology

To identify and exclude faulty satellites, the proposed FDE method uses a main IF and a bank of sub-filters. The figure 1 shows the block diagram of the proposed approach. The diagram is composed of five parts. The first part is the observations acquisition. Then, marginalization stage is applied on both, information vector and information matrix. The IF prediction comes in the third step (equations 13 to 17 are used for such prediction).

The proposed FDE approach is represented and explained in Figure 2. The approach consists of three stages. The main IF and different information sub-filters are synthetized. Then, the Likelihood test (LLT) (equation 24 and 25) compares the certainty of each sub-filter with the certainty of the main filter. The LLT changes will attempt to detect the CS.

The final part of the proposed approach is the "update step" which is used in order to obtain a more accurate estimation.

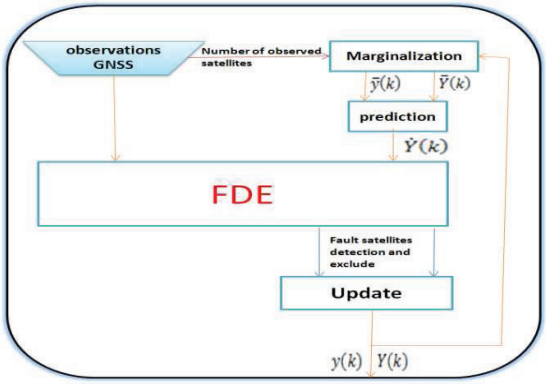

Figure 1: The proposed methodology

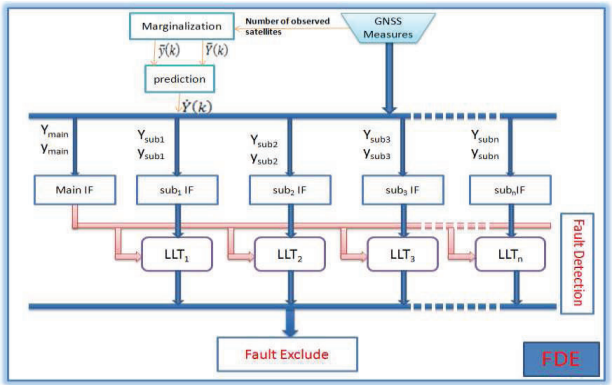

Figure 2: Block diagram of the proposed Fault Detection Exclusion method

4 Results and Discussions

To examine the performance of the proposed FDE approach, a data acquisition has been carried out at the CRIStAL laboratory in Lille I University. The CyCab vehicle produced by the Robosoft company (www.robosoft.fr) is used with an open GPS system (ublox EVK-6T-open). The test trajectory showed in figure 4 is about 1073 meters (189 epochs). During these experiments, we deliberately choose a constraint area to obtain the Non Line of Sight (NLOS) phenomena.

As shown in figure 3 (the red line), when the positioning system takes in consideration all visible satellites without an FDE stage, a bias in the positioning process is observed specially near to the trajectory section surrounded by trees and nearby building.

To examine the capacity of LLT to detect different types of observation errors, a reference trajectory is needed. In this work, a GPS RTK (Thales Sagitta 02) positioning system is used with a corrected test trajectory in order to compute the observation errors. Knowing the reference trajectory, one can calculate the real error of observations ρ and φ of all satellites at instant k represented respectively by $real\_R_{\rho}^{si}(k)$ and $real\_R_{\varphi}^{si}(k)$. We can also estimate the real distance between the satellite i and the receiver at instant k represented by $p_r^{si}(k)$.

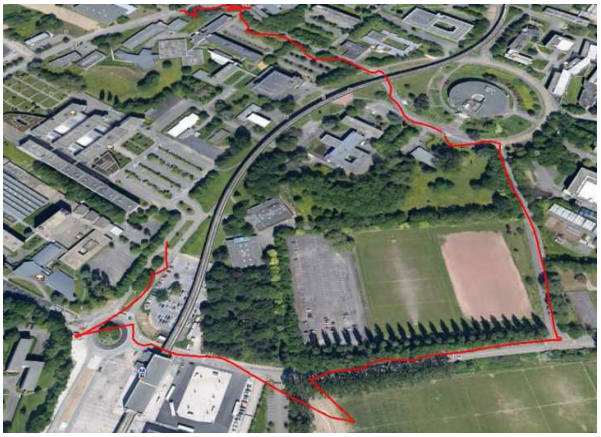

Figure 3: trajectory before FDE

$real\_R_{\rho}^{si}$ is calculated as the difference between $p_r^{si}(k)$ and $\rho_r^{si}(k)$ while $\text{real\_R}_{\varphi}^{si}$ as the difference between $p_r^{si}(k)$ and $\varphi_r^{si}(k)$. $\text{real\_R}_{\rho}^{si}$ and $real\_R_{\varphi}^{si}$ equations can be written as:

$$p_r^{si}(k) = \sqrt{[(x_i^s(k) - x_{RTK}(k))^2 + (y_i^s(k) - y_{RTK}(k))^2 + ((z_i^s(k) - z_{RTK}(k))^2]} \quad (30)$$

$$real_{R_{\rho}}^{si}(k) = p_r^{si}(k) - (\rho_r^{si}(k) + Ion_r^{si}(k) + T_r^{si}(k) + c\left(\partial_r(k) - \partial^{si}(k)\right)) \quad (31)$$

$$real_{R_{\phi}}^{si}(k) = p_r^{si}(k) - (\lambda\,\varphi_r^{si}(k) + \lambda\,\tilde{N}_r^{si}(k) - Ion_r^{si}(k) + T_r^{si}(k) + c\left(\partial_r(k) - \partial^{si}(k)\right)) \quad (32)$$

Where $(x_i^s(k), y_i^s(k), z_i^s(k))$the coordinates of are satellite 'i' at instant k, $(x_{RTK}(k), y_{RTK}(k), z_{RTK}(k))$ are the receiver's coordinates at instant k estimated by a corrected GPS RTK. $real\_R$ can reflect the existence of observation error. In observation of several experimentations and using simulation data, one can remark that the sudden changes and high amplitude in $real\_R_{\varphi}$ is an indication of the presence of cycle slips on the φ observation.

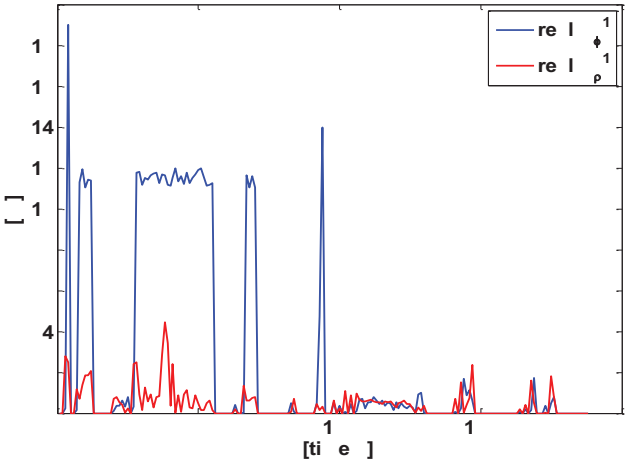

Figure 4.a: the $real\_R_{\varphi}$ and $real\_R_{\rho}$ of satellite 21

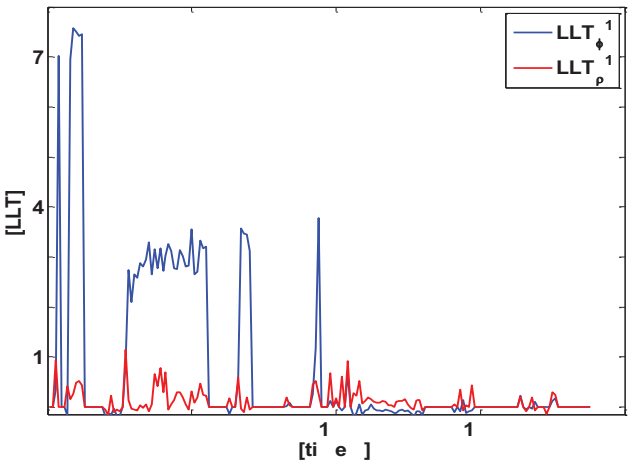

Figure 4.b: the LLT^{φ} and LLT^{ρ} of satellite 21

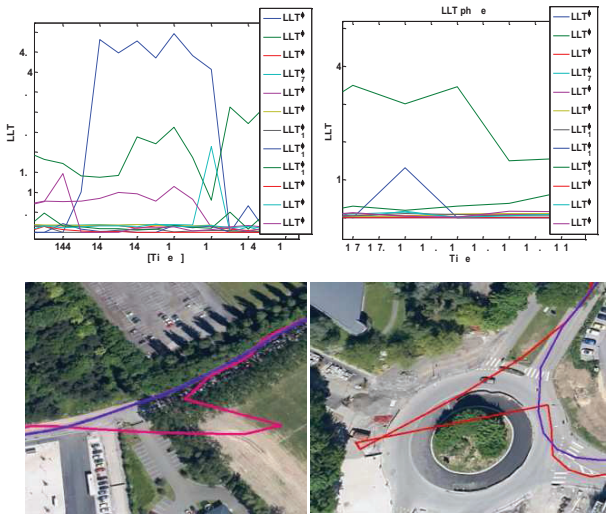

Figure 4.c : all LLT^{φ} for the sections of test trajectory encircled

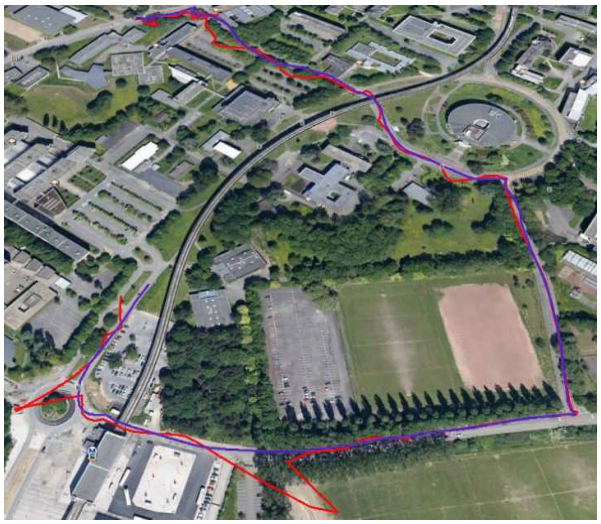

Figure 4.d: trajectory after FDE

Figure 4.a present $real\_R_{\varphi}$ and $real\_R_{\rho}$ of satellite 21 and 4.b show the LLT_{φ} and LLT_{ρ} of satellite 21. We observe a prominent peak appears with $real\_R_{\varphi}$ and LLT_{φ} (at instant 4, 28 to 54, 67 to 70 and 91), when no peaks appear with $real\_R_{\rho}$ and LLT_{ρ}. One can conclude that the high LLT_{φ} values could be considered as CS and thus the results show the capability of LLT_{φ} to detect such errors.

Figure 4.c shows the value of LLT^{φ} for all satellites observed during two sections encircled in the test trajectory (figure 4.d) and the corresponding trajectory result of these sections before excluding (red line) and after excluding (blue line) the faulty measurements. The LLT^{φ} increase strongly for satellites 3, 13, and 26 in the section encircled by a yellow circle. In the second section (black circle), the same conclusion can be made for satellite 2 and 13.

Figure 4.d show the performance and accuracy of the proposed method (FDE method).

5 Conclusion and Future works

GNSS measurements cannot provide a high integrity and desirable precision. For this reason since several years, researchers try to develop methods that improve the integrity and the precision of GNSS measurements. In this paper, we proposed a new method for detecting and exclude the CS of the carrier phase measurements and other kind of faults of the GNSS measurements. It is based on the use of IF to estimate the position and information test to compare the certainty of a main filter in comparison to a bank of sub filters. The method was tested with real data. Performances are illustrated giving a high integrity

positioning and improving the accuracy of localization using C/A code and carrier phase measurements.

Furthermore; as future works, we aim to study the multi-fault detection and multi-cycle-slips by using multiple GNSS systems to improve the performance and integrity of positioning. For example, using both GPS Ll/L2 and GLONASS Ll/L2 signals. In addition, we study the use of 3D city model in order to detect the NLOS and multipath of GNSS measurements.

References

[1] A. Simsky, "Standalone real-time navigation algorithm for single-frequency ionosphere-free positioning based on dynamic ambiguities (DARTS-SF)," in Proceedings of the ION GNSS 18th International Technical Meeting of the Satellite Division, Fort Worth, Texas, 2006, pp. 301–308.

[2] K. Chen and Y. Gao, "Real-time precise point positioning using single frequency data," in ION GNSS, 2005.

[3] B. Wang, D. Chen, and H. Bian, "Cycle Slips Detection and Repairing to GPS Phase Observation Based on Sym4 Wavelet," in 2011 International Conference on Multimedia and Signal Processing (CMSP), 2011, vol. 1, pp. 329–333.

[4] T. Yi, H. Li, and G. Wang, "Cycle Slip Detection and Correction of GPS Carrier Phase Based on Wavelet Transform and Neural Network," in Sixth International Conference on Intelligent Systems Design and Applications, 2006. ISDA '06, 2006, vol. 1, pp. 46–50.

[5] L. Gun, H. Yong-Hui, and Z. Wei, "A New Algorithm of Detecting and Correction Cycle Slips in Dual-Frequency GPS," in 2006 IEEE International Frequency Control Symposium and Exposition, 2006, pp. 622–627.

[6] S. Feng, W. Ochieng, T. Moore, C. Hill, and C. Hide, "Carrier phase-based integrity monitoring for high-accuracy positioning," GPS Solut., vol. 13, no. 1, pp. 13–22, Jan. 2009.

[7] M. Kirkko-Jaakkola, J. Traugott, D. Odijk, J. Collin, G. Sachs, and F. Holzapfel, "A raim approach to GNSS outlier and cycle slip detection using L1 carrier phase time-differences," in IEEE Workshop on Signal Processing Systems, 2009. SiPS 2009, 2009, pp. 273–278.

[8] D.-J. Lee, "Nonlinear estimation and multiple sensor fusion using unscented information filtering," Signal Process. Lett. IEEE, vol. 15, pp. 861–864, 2008.

[9] S. Grime and H. F. Durrant-Whyte, "Data fusion in decentralized sensor networks," Control Eng. Pract., vol. 2, no. 5, pp. 849–863, 1994.

[10] N. A. Tmazirte, M. E. E. Najjar, C. Smaili, and D. Pomorski, "Multi-sensor data fusion based on information theory. Application to GNSS positionning and integrity monitoring," in 2012 15th International Conference on Information Fusion (FUSION), 2012, pp. 743–749.

[11] E. Realini and M. Reguzzoni, "goGPS: open source software for enhancing the accuracy of low-cost receivers by single-frequency relative kinematic positioning," Meas. Sci. Technol., vol. 24, no. 11, p. 115010, Nov. 2013.

[12] R. M. Eustice, H. Singh, and J. J. Leonard, "Exactly Sparse Delayed-State Filters for View-Based SLAM," IEEE Trans. Robot., vol. 22, no. 6, pp. 1100–1114, Dec. 2006.

[13] P. Ahrendt, "The multivariate gaussian probability distribution," 2005.

[14] S. Thrun, Y. Liu, D. Koller, A. Y. Ng, Z. Ghahramani, and H. Durrant-Whyte, "Simultaneous Localization and Mapping with Sparse Extended Information Filters," Int. J. Robot. Res., vol. 23, no. 7–8, pp. 693–716, Aug. 2004.

[15] X. Xiang Jin and C. D. de Jong, "Relationship Between Satellite Elevation and Precision of GPS Code Observations," J. Navig., vol. 49, no. 02, pp. 253–265, 1996.

[16] L. Ciraolo, F. Azpilicueta, C. Brunini, A. Meza, and S. M. Radicella, "Calibration errors on experimental slant total electron content (TEC) determined with GPS," J. Geod., vol. 81, no. 2, pp. 111–120, 2007